

SUPPLEMENTARY INFORMATION

Experimental procedures

H/D exchange

For H/D exchange measurements NMR buffer was lyophilized twice and re-dissolved in D₂O (99.9%). The buffer exchange from a H₂O- to a D₂O-containing buffer of the SpaI sample was done using a PD-10 desalting column (GE Healthcare) according to the manufacturer's instructions. ¹⁵N-HSQC spectra were recorded after 1 h, 1 h 45 min, 2 h 25 min, 5 h 45 min, 2 d 13 h and 3 d 6 h.


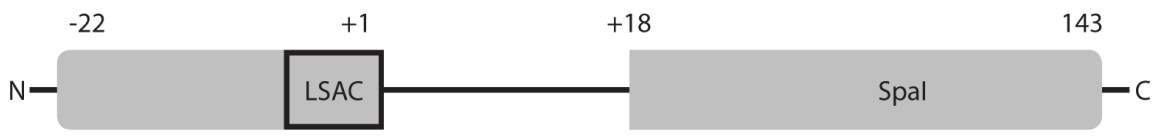
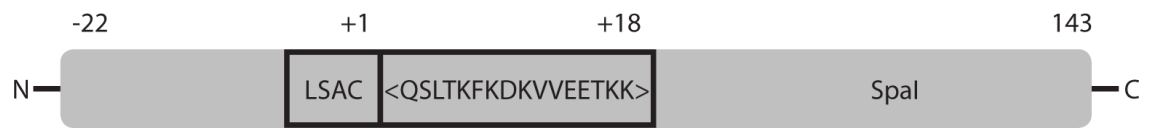



Site directed spin labeling of SpaI mutants

The wild type SpaI sequence does not contain any native cysteines, therefore three cysteine residues were introduced in SpaI₁₈₋₁₄₃ (S30C, K62C and S94C). The positions for the single-cysteine mutations were chosen based on our preliminary structural data. The mutants were expressed overnight at 37 °C using M9 minimal media containing 1 g/l ¹⁵NH₄Cl (Cambridge Isotope Laboratories). The purification protocol established for SpaI constructs was used (see Materials and Methods) with the addition of 2 mM β-mercaptoethanol in all buffers. The samples were divided after anion exchange chromatography. One half was subjected to normal gel filtration while the other half was used in the spin labeling reaction. In brief, buffer was exchanged to a non-reducing environment (25 mM HEPES, 100 mM NaCl, pH 7.0) via a PD-10 desalting column (GE Healthcare). A 10 fold excess of the spin-label 4-maleimido-TEMPO (Sigma-Aldrich) was incubated with the protein for 2 h at RT. Gel filtration with the column equilibrated in NMR buffer (50 mM sodium phosphate, 100 mM NaCl, pH 6.4) was used to remove excess spin label.

Homology models of EtnI and EriI

Homology models of EtnI and EriI were generated using the SWISS-MODEL Server (1) in the automated mode providing the mean structure of SpaI₁₈₋₁₄₃ as template. The sequence alignment of full-length SpaI to EtnI and EriI is shown in Figure 1.

TABLE S1. *B. subtilis* strains used in this study.

Strains	Characteristic or description ^b	Source or reference
B15029	Wild type; (Etn ⁺)	Laboratory stock
B2470	CU1065 <i>liaI</i> :pMUTIN; erythromycin resistance	(2)
B2470.SD3	B2470 <i>amyE</i> :: <i>cat</i> (Etn ⁻)	(3)
B2470.SD4 (NisI WT)	B2470 <i>amyE</i> ::[P _{xyI} - <i>nisI</i> ((-16,(+)226) <i>cat</i>] (Etn ⁻)	This work
		
B2470.SB2 (SpaI(Δ2-17))	B2470 <i>amyE</i> ::[P _{xyI} - <i>spaI</i> ((-22,(+)143, Δ2-17) <i>cat</i>] (Etn ⁻),	This work
		
B2470.SB3 (SpaI WT)	B2470 <i>amyE</i> ::[P _{xyI} - <i>spaI</i> ((-22,(+)143) <i>cat</i>] (Etn ⁻),	This work
		
B2470.SB7 (SpaI-Scramble)	B2470 <i>amyE</i> ::[P _{xyI} - <i>spaI</i> ((-22,(+)143, <2-vfkdttsklqkvkeke-17>) <i>cat</i>] (Etn ⁻)	This work
		
B2470.SB8 (EtnI WT)	B2470 <i>amyE</i> ::[P _{xyI} - <i>etnI</i> ((-48,(+)143) <i>cat</i>] (Etn ⁻)	This work
		
B2470.SB17 (SpaI-Negative)	B2470 <i>amyE</i> ::[P _{xyI} - <i>spaI</i> ((-22,(+)143, <2-qsItefedsvveetee-17>) <i>cat</i>] (Etn ⁻)	This work
		

^a Etn⁺ or Etn⁻ stands for entianin producing or non-producing strain.

^b Numbers following *lanI* genes indicate the included amino acids of the encoded protein. Brackets <...> indicate sequence mutations compared to the WT sequence, whereas the numbers at the beginning and end of the brackets correspond to the first and last amino acid mutated, respectively.

TABLE S2. Ten best results from the DALI-server search for homologous structures (4).

rank	pdb code	Z-score	rmsd	# of aligned positions	# of residues in matched structures	sequence identity [%]	description
1	3hbl-D	2.5	11.7	64	1067	9	MOLECULE: PYRUVATE CARBOXYLASE;
2	3bg5-D	2.5	11.2	62	1067	8	MOLECULE: PYRUVATE CARBOXYLASE;
3	2dc4-A	2.4	4.5	78	164	10	MOLECULE: 165AA LONG HYPOTHETICAL PROTEIN;
4	3bg3-A	2.4	3.4	56	680	14	MOLECULE: PYRUVATE CARBOXYLASE, MITOCHONDRIAL;
5	2dc4-B	2.4	4.5	78	164	10	MOLECULE: 165AA LONG HYPOTHETICAL PROTEIN;
6	2qf7-A	2.4	11.5	63	1076	14	MOLECULE: PYRUVATE CARBOXYLASE PROTEIN;
7	2qf7-B	2.4	11.9	60	1016	13	MOLECULE: PYRUVATE CARBOXYLASE PROTEIN;
8	3tw7-B	2.4	12.1	60	1011	15	MOLECULE: PYRUVATE CARBOXYLASE PROTEIN;
9	3bg5-B	2.4	12.8	64	1074	6	MOLECULE: PYRUVATE CARBOXYLASE;
10	3bg5-C	2.4	10.2	61	1067	8	MOLECULE: PYRUVATE CARBOXYLASE;

= number

SUPPLEMENTAL FIGURES

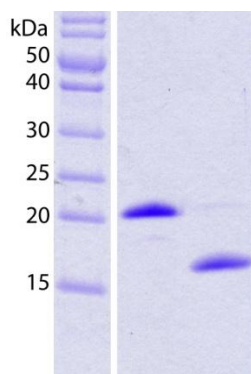


FIGURE S1. SDS-PAGE of the trypsin digest of SpaI₃₋₁₄₃.

Trypsin digest of 4 μ g SpaI₃₋₁₄₃ (lane 1) with 0.2 μ g trypsin (4 h at 16 °C) resulted in an approximately 15 kDa stable fragment of SpaI (lane 2). MALDI-MS analysis identified this fragment to be the C-terminal fragment SpaI₁₈₋₁₄₃ which was subsequently used for structure determination.

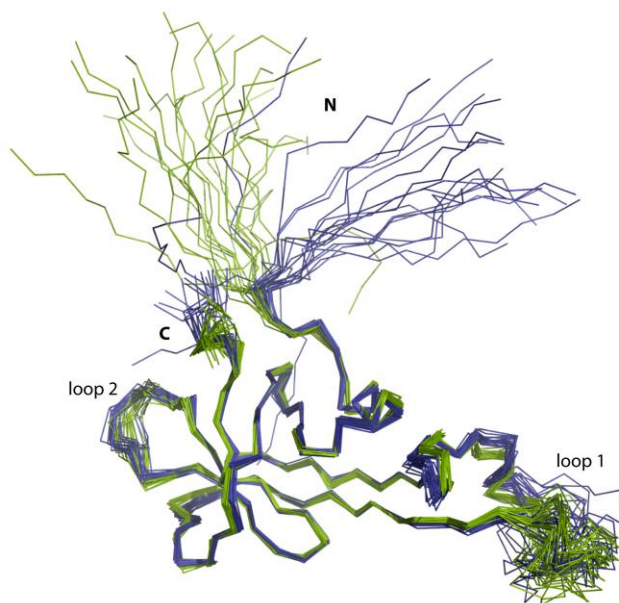


FIGURE S2. Influence of RDCs on the results of the structure calculation.

Superposition of the C α atoms of ordered residues of the 20 lowest energy conformers of SpaI calculated without (blue) and with (green) RDCs.

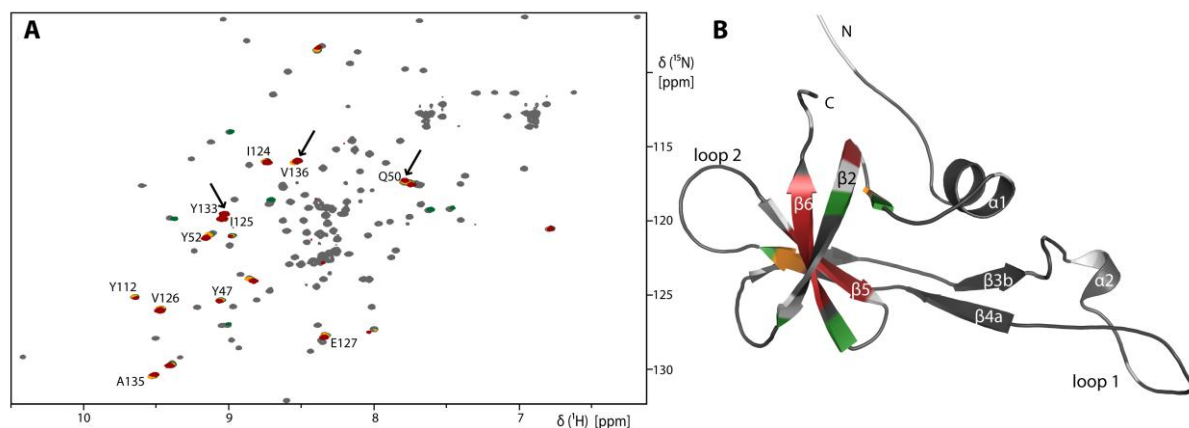


FIGURE S3. H/D exchange.

A. Overlay of $[^1\text{H}, ^{15}\text{N}]$ -HSQCs showing amide resonances which did not exchange with D_2O after 5 h 45 min (green), 2 d 13 h (orange) and 3 d 6 h (red). A reference $[^1\text{H}, ^{15}\text{N}]$ -HSQC recorded in H_2O is shown in grey. Arrows indicate signals of amides for which hydrogen bond restraints were added to the structure calculation. Other assigned signals are amides for which hydrogen bonds were already directly detected in the long-range HNCO. **B.** Residues whose amides did not exchange are mapped onto the structure and colored according to **A**. Residues colored white are prolines or resonances that could not be tracked reliably due to resonance overlap. The structure does not show the entire N-terminus.

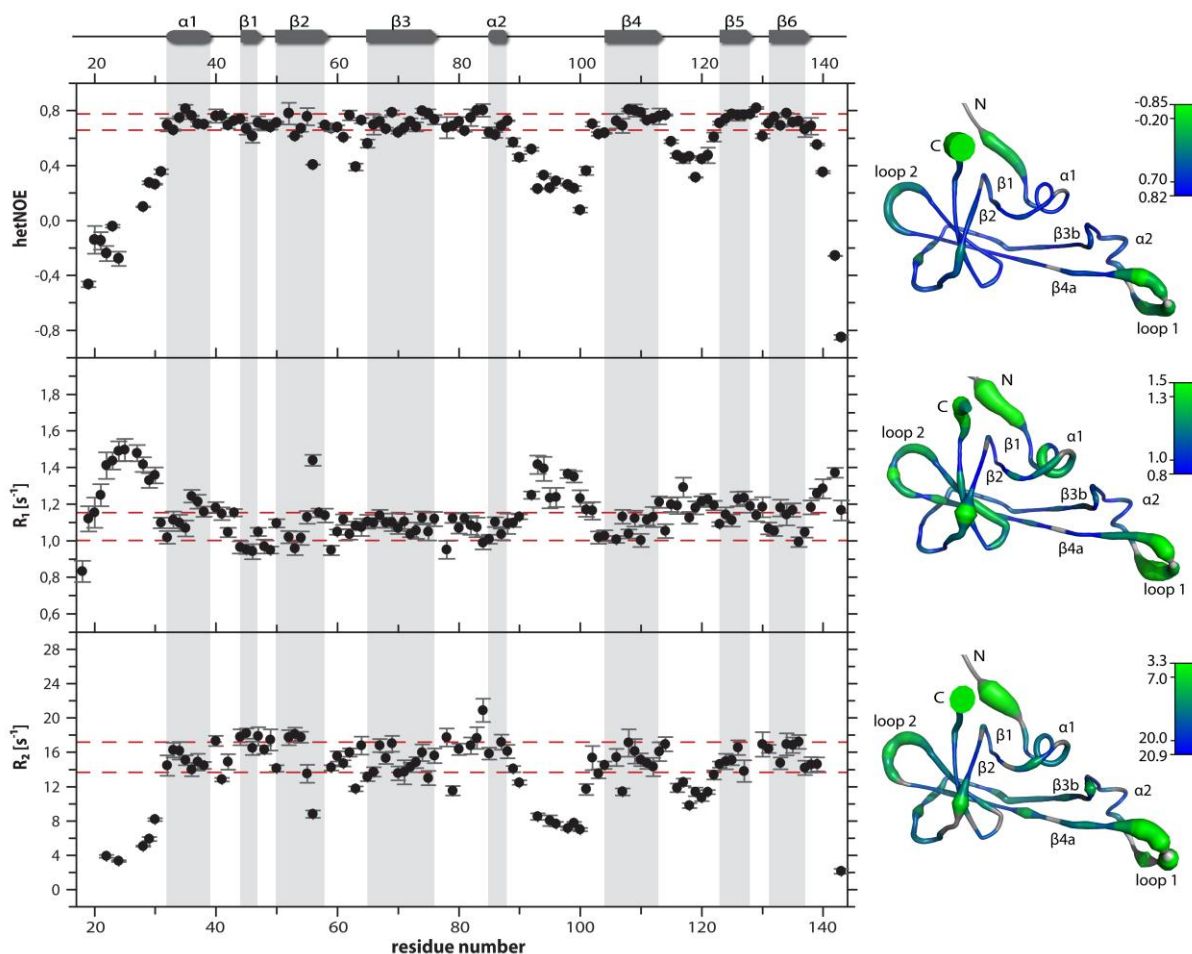


FIGURE S4. Internal dynamics of SpaI₁₈₋₁₄₃.

$\{^1\text{H}\}$, ^{15}N -HetNOE, R_1 and R_2 relaxation rates of the backbone amides of SpaI₁₈₋₁₄₃ are plotted against the sequence. The secondary structure is shown above and indicated throughout the plots as grey columns. Between the red dotted lines are values for rigid parts of the protein drawn from the standard deviation of N-H vectors with HetNOE values above 0.6. Values are plotted onto the structure (showing amino acids 25-143) next to each plot. Green thick tubes or blue thin tubes represent flexible or rigid parts of the structure, respectively. In detail high HetNOE and R_2 values are indicated by thin blue tubes and low values are represented by thick green tubes. For R_1 relaxation rates the color-coding schema and the tube thickness are reversed. Missing data points in the plots and grey thin tubes in the structure indicate prolines or values that could not be determined reliably.

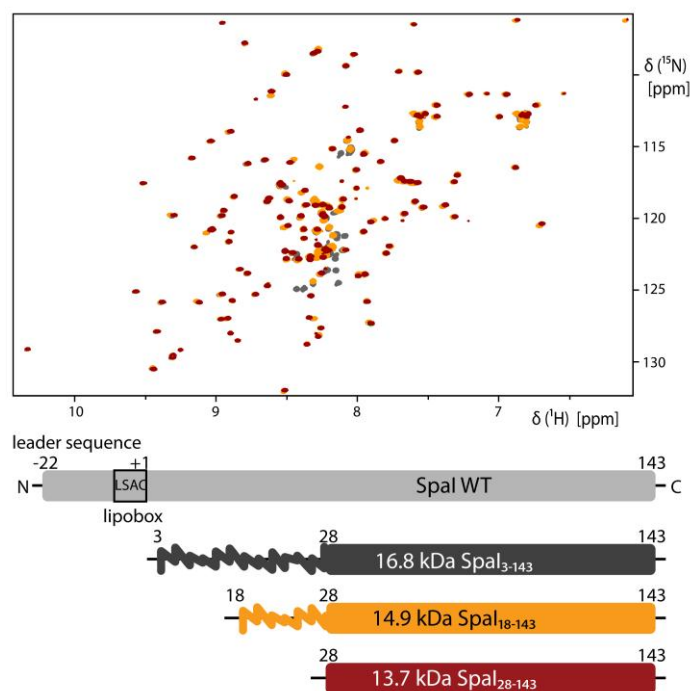


FIGURE S5. [^1H , ^{15}N]-HSQCs of SpaI NMR constructs.

An overlay of the [^1H , ^{15}N]-HSQC-spectra of three different constructs of SpaI (color coded according to the cartoon representation below) is shown. In analogy to Figure 2 an even shorter construct of SpaI (SpaI₂₈₋₁₄₃) shown in red adopts an identical structure in solution as indicated by the virtually identical spectra. $\{^1\text{H}\}$, ^{15}N -HetNOE data (see Fig. 3) revealed amino acids 18-28 of SpaI₁₈₋₁₄₃ (orange) as flexible in addition to the first 15 amino acids of the longer construct ranging from amino acid 3 to 143 (represented in black). Therefore the SpaI₂₈₋₁₄₃ construct represents the structured part of SpaI and was used for recording the long-range HNCO-experiment.

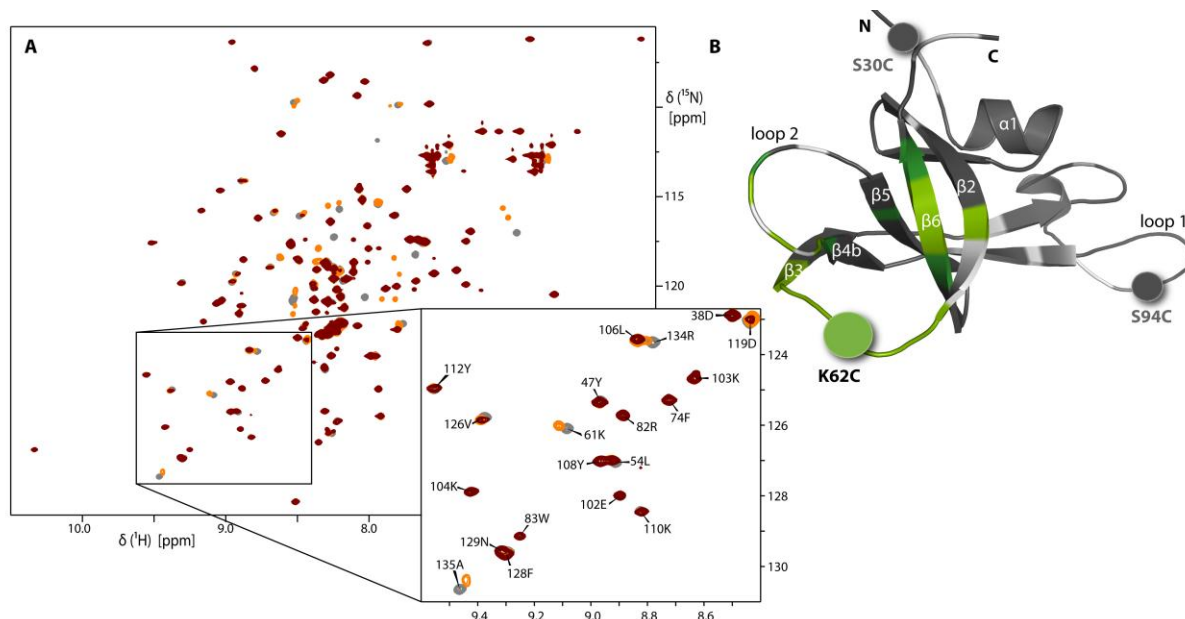


FIGURE S6. PRE measurement of K62C SpaI₁₈₋₁₄₃.

A. An overlay of $[\text{}^1\text{H}, \text{}^{15}\text{N}]$ -HSQCs indicating backbone amide signals affected by the presence of a 4-maleimido-TEMPO spin label at position 62 is shown. The reference spectrum of the K62C mutant without the spin-label is shown in grey and spectra prior to and after reduction of the spin label are colored in red and orange, respectively. **B.** Residues whose signal intensity is affected by the spin label at position K62C are mapped onto the structure. For analysis, signals of the $[\text{}^1\text{H}, \text{}^{15}\text{N}]$ -HSQCs in A were separated into four groups; light green: resonance is broadened completely, dark green: resonance with lower intensity than reference, grey: resonance with no intensity change compared to reference, white: positions of prolines or resonances that could not be unambiguously identified due to overlap. The position of the spin label is indicated in the structure by a green sphere (structure does not show the full N-terminus). Spin-label positions for the other two SpaI mutants (S30C and S94C) are shown by grey spheres together with their residue numbers.

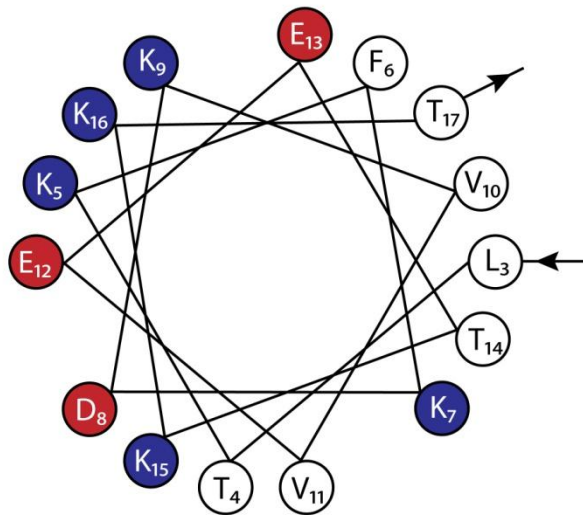


FIGURE S7. The N-terminal amino acids of SpaI have the potential to form an amphipathic α -helix.

Helical wheel drawing of the N-terminal amino acids 3-17 of SpaI. Amino acids are colored according to their charge: blue for positive, red for negative and white for non-charged amino acids. A α -helix is predicted for amino acids 3 to 15 e. g. by the secondary structure prediction program PSIPRED (5).

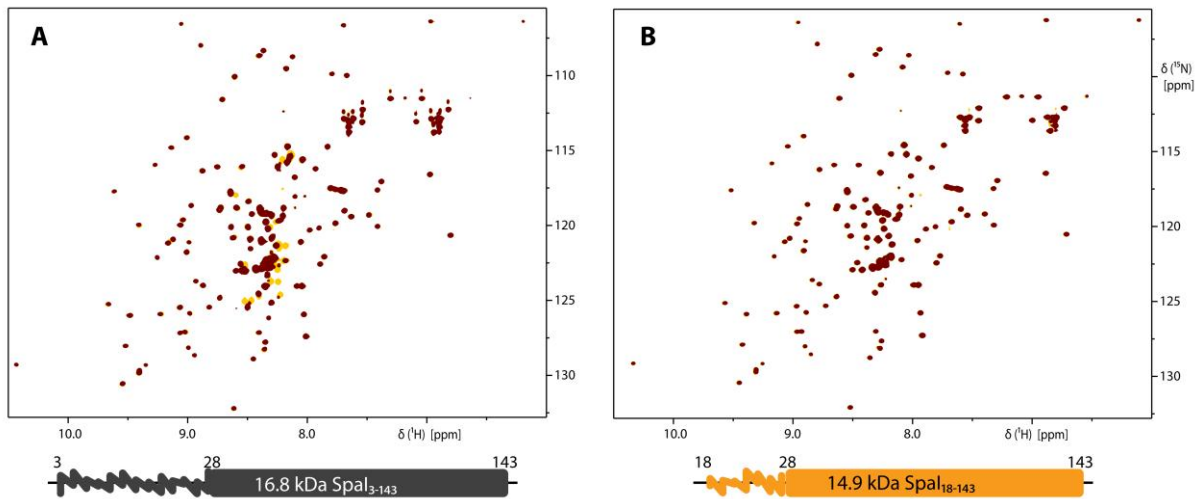


FIGURE S8. Titration of multilamellar liposomes to SpaI constructs.

A and **B**. Overlay of $[^1\text{H}, ^{15}\text{N}]$ -HSQCs of SpaI₃₋₁₄₃ (**A**) and SpaI₁₈₋₁₄₃ (**B**) in absence (yellow) and presence of liposomes (red) is shown (liposomes prepared from DOPG, DOPE and CL in the molar ratio of 3:2:3 to mimic the native membrane of *B. subtilis*). SpaI concentrations are 0.1 mM, lipid concentration for **A** is 5 mM and 25 mM for **B**. Schematics of SpaI constructs used for the lipid titrations are shown below the corresponding spectrum.

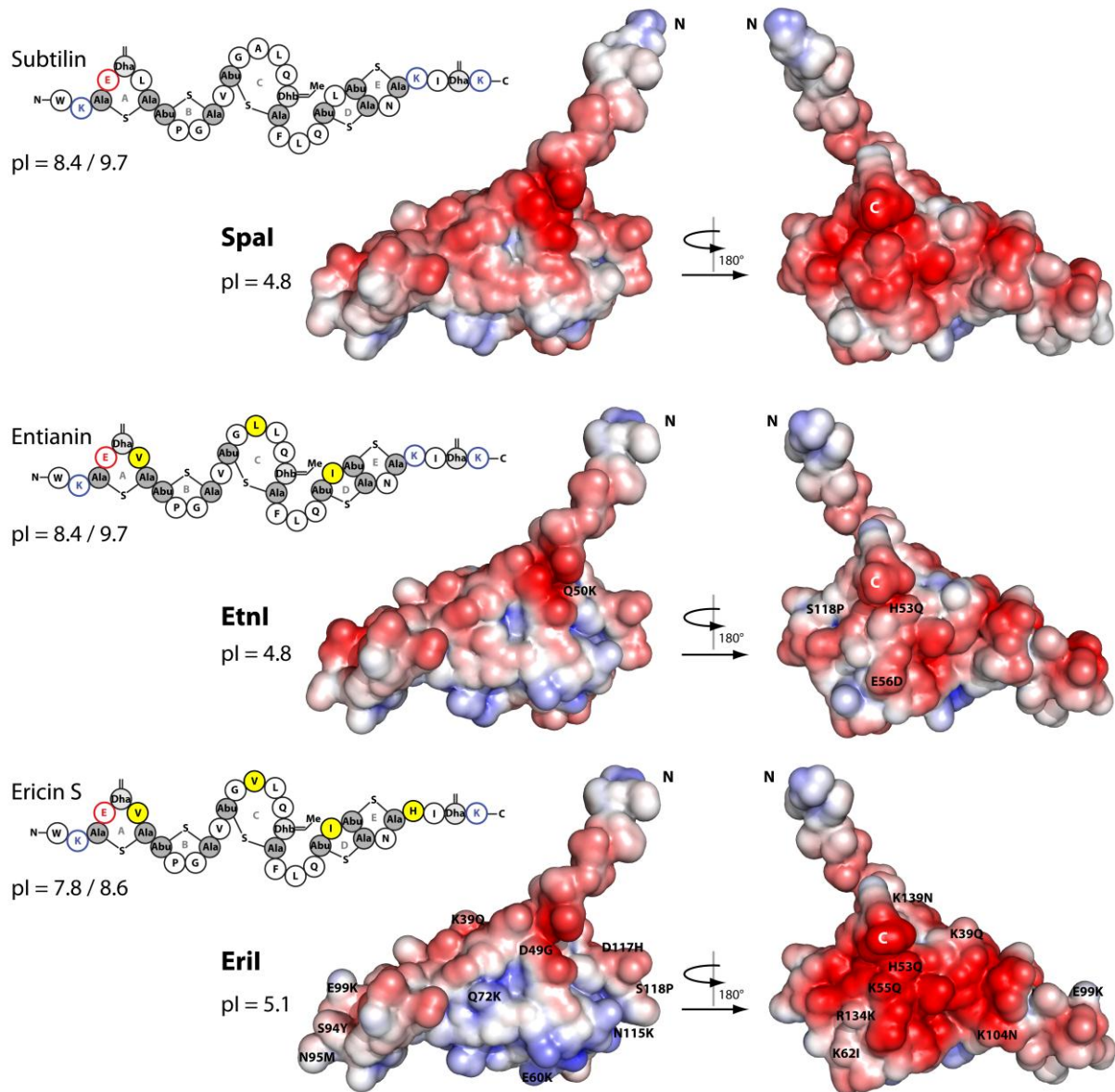


FIGURE S9. Homology of SpaI to its close relatives EntI and EriI

Electrostatic surface potential mapped on the solvent accessible surface of SpaI₁₈₋₁₄₃ and homology models of EntI₁₈₋₁₄₃ and EriI₁₈₋₁₄₇ showing from red ($-5 kT/e$) to blue ($+5 kT/e$) negatively to positively charged residues, respectively (k = Boltzmann's constant, T = absolute temperature and e = electron charge). The left surface of SpaI is oriented towards the periplasm whereas the right surface represents the membrane proximal side. The primary structures of the corresponding lantibiotics are shown next to the homology models of their corresponding LanI proteins. Differences in lantibiotic sequence are highlighted in yellow and charged residues are color-coded. Calculated isoelectric points of the LanI proteins (starting at the lipid anchored cysteine) and lantibiotics (using either the sequence of pre-subtilin (first value) or substituting all serine, threonine and cysteine residues with alanine (second value)) calculated with the ProtParam (6) tool are indicated.

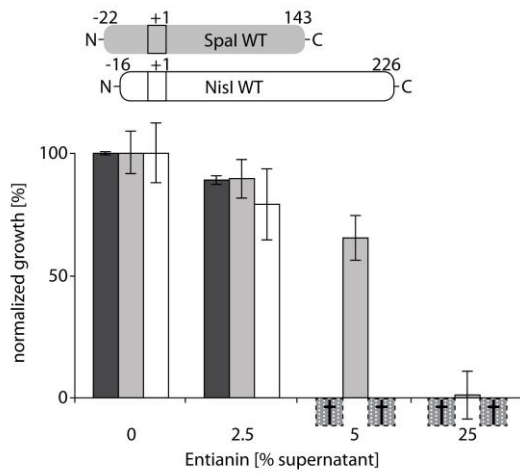


FIGURE S10. NisI does not confer immunity against entianin.

Percental growth increase after 1 hour incubation with entianin (% supernatant) normalized to the control without lantibiotic. Black bars: control-strain B2470.SD3 without any *lanI* gene, grey bars: the Spal WT expressing strain B2470.SB3 and white bars: the NisI WT expressing strain B2470.SD4. Negative bars indicate cell lysis and their height is set to an arbitrary value. The sketches above the bars represent the respective LanI-variant.

REFERENCES

1. Schwede, T., Kopp, J., Guex, N., Peitsch, M. C. (2003) SWISS-MODEL: An automated protein homology-modeling server. *Nucleic Acids Res.* **31**, 3381–3385
2. Mascher, T., Zimmer, S. L., Smith, T.-A., Helmann, J. D. (2004) Antibiotic-inducible promoter regulated by the cell envelope stress-sensing two-component system LiaRS of *Bacillus subtilis*. *Antimicrob. Agents Chemother.* **48**, 2888–2896
3. Fuchs, S. W., Jaskolla, T. W., Bochmann, S., Kötter, P., Wichelhaus, T., Karas, M., Stein, T., Entian, K.-D. (2011) Entianin, a novel subtilin-like lantibiotic from *Bacillus subtilis* subsp. *spizizenii* DSM 15029T with high antimicrobial activity. *Appl. Environ. Microbiol.* **77**, 1698–1707
4. Holm, L., Rosenström, P. (2010) Dali server: conservation mapping in 3D. *Nucleic Acids Research.* **38**, W545–W549
5. Buchan, D. W. A., Ward, S. M., Lobley, A. E., Nugent, T. C. O., Bryson, K., Jones, D. T. (2010) Protein annotation and modelling servers at University College London. *Nucleic Acids Res.* **38**, W563–8
6. Gasteiger, E., Hoogland, C. G. A., Duvaud, S., Wilkins, M., Appel, R., Bairoch, A., in: Walker J.M. (Ed.) (2005) *The Proteomics Protocols Handbook*, Humana Press, pp. 571–607